MANAS Journal of Engineering
ISSN 1694-7398 | e-ISSN 1694-7398

Volume 9, Issue 1, (2021) Pages 37-44
https://doi.org/10.51354/mjen.854265

A Gas Sensor Design and Heat Transfer Simulation with ZnO and TiO_2 Sensing Layers

Gozde Konuk Ege[1,*], Huseyın Yuce[2], Garıp Genc[3]

[1] Istanbul Gedik University, Istanbul, 34913, Turkey, gozde.konuk@gedik.edu.tr, ORCID: 0000-0001-7349-0416

[2] Marmara University, Istanbul, 34722, Turkey, huseyin@marmara.edu.tr, ORCID: 000-0001-5525-7733

[3] Marmara University, Istanbul, 34722, Turkey, ggenc@marmara.edu.tr, ORCID: 0000-0001-7711-3845

ABSTRACT

Micro Electro-Mechanical System (MEMS) based devices offer innovative approaches in sensor technologies with the advantages of high efficiency and miniaturization. The most important stage in the development of new generation MEMS-based devices is the design and optimization stage. However, device design and optimization processes are developed in a laboratory by empirical approaches. This causes time loss and creates an unnecessary waste of resources. In this study, it is aimed to design and analyze two gas sensors based on ZnO and TiO_2 sensing layers. Electro-thermal analysis of the sensor structure was carried out at room temperature and high temperature (294,15K-573,15K) and heat transfer parameters were compared. According to the simulation results, it is obtained that, as the applied temperature increases to the sensor, the temperature over the sensing layer increases linearly. It is compatible with the literature. The temperature on the ZnO surface increases to three times the TiO_2 surface temperature. The heat transfer results obtained will be used as a guide for device design and optimization in future works. In this way, as a result of numerical analysis, a MEMS-based device will be produced with high accuracy. Thus, time and resources will be saved.

ARTICLE INFO

Research article

Received: 5.01.2021
Accepted: 30.04.2021

Keywords:
gas sensor,
sensing layer,
finite element method
(FEM,heat transfer)

*Corresponding author

1 Introduction

Rapidly increasing environmental pollution and consequently increasing health problems have become one of the most important problems of today. In addition, different gases are frequently used in the manufacturing industry. This situation directly affects to human health. The integration of smart devices developed for the benefit of humanity into our daily life is becoming more and more popular with decades due to their usefulness. Gains in MEMS technology also has been affected sensor technologies. Sensors produced in line with micro technologies have advantages in terms of cost, miniaturization, and sensitivity as smart sensors. In this view, the development of gas detection devices is important for widespread uses, such as monitoring gas accumulation, medical diagnostics, food quality assurance and the safety of industrial processes or domestic systems. Today, in parallel with the technological progress in nano-electronic structuring and the point it has reached, gas sensor technologies continue to progress with similar acceleration [1–5].

Micro/nano technology is a multi-disciplinary technology because of using material science, structure-control design and finite-element method (FEM). Material technology allows the use of new generation materials and semiconductor technologies in miniature device development. Moreover, structural/control design and analysis methods offer high accuracy and analysis advantages with high accuracy.

It was observed for the first time in 1953 that the conductivities of semiconductor materials are changed by gas absorption [6]. Subsequently, the first semiconductor gas sensor patented in 1962 [7]. Afterwards, gas-sensing devices are researched and examined worldwide. Researches on gas detection mechanisms is focused on designing gas detection elements that can detect gases harmful to human health and nature with high performance detection materials as a consequence various gas detection technologies have been developed for use in gas detection processes [8–13].

Table 1. *Gas detection methods used in gas detection processes*

Gas sensors related to detecting material	Gas sensors related to detecting mechanism
Metal oxide semiconductors	Resistance Change
Carbon nanotubes	Optical methods
Polymers	Acoustic methods
	Gas chromatography
	Calorimetric methods

Gas detection processes can be examined in two classes, according to the sensing material and the sensing mechanism, as shown in Table 1. In gas sensors; Metal oxide semiconductors, carbon nanotubes and polymers are used as the material in the gas detection layer. On the other hand, resistance changing, optical methods, acoustic methods (eg; SAW sensor), calorimetric method and gas chromatography can be used as the detection mechanism. Metal oxide-based gas sensors attract researchers' attention thanks to their high detection capability, repeatability and simple manufacturing techniques. MO_X-based gas sensors are used to sense NH_3, H_2, NO_2, H_2S, CO, CO_2, SO_2, O_3, N_2, VOCs, LPG gases [14].

NH_3, H_2, HCl, NO_2, H_2S, CO, CO_2 gases threat human health depending on their conditions of use and release rates of these gases. Table 2 presents that the areas of use or release of these gases and their danger. For example; NH_3 gas appears in the chemical, food and health industry and causes a toxic effect. NO, HCl, CO_2 gases cause respiratory disorders. The release of high levels of H_2S and CO, H_2 gases can result in death.

The working principle of MO_X gas sensors are usually based on the resistivity change of the semiconductor, depending on the gas absorption. When gas analytes come into contact with the sensing layer, the adhesion of oxygen atoms occur on the surface and semiconductor sensing material reacted to the gas analytes. In this way, sensing layer resistivity is decreased according to the analyte concentration. However, the worst feature of MOx-based gas sensors is that they have a high operating temperature. This situation requires high power consumption and an external heat source [33]. Therefore, many studies are carried out to obtain high operating performance at low temperatures. In this study, two MOx-based gas sensors model are designed.

Table 2. *According to the encountered area, and their dangers various hazardous gases*

Hazardous Gases	**The encountered Area**	**Dangers**
NH_3 [15]	Chemical and food industry, medical diagnosis	Toxic effect, vomiting, headache
NO [16–19]	Combustion of fossil fuels, power plants and vehicle engines	Respiratory diseases, asthma
NO_2 [20]	Automobile exhaust fumes, nitric acid production, coal and fuel combustion	Acid rain, environmental pollution
H_2 [21–25]	Renewable energy sources, transport systems and biomedical devices	Explosive, flammable
H_2S [26–29]	Oil/natural gas, geothermal energy and bacterial decomposition	Occupational diseases, death in high concentration
HCl [30]	Semiconductor and chemical industry	Toxic effect, skin burns, respiratory disorders
CO [31]	Fire events	Toxic effect , death
CO_2 [32]	Cellular respiration and burning of fossil fuels	Respiratory disorders, explosion, Global warming, explosion

One of the gas sensors consists of TiO_2 as a sensing layer and another is consist of ZnO. Three-dimensional design and simulation are done by using SolidWorks and COMSOL Multiphysics software. The electro-thermal analysis is done to observe the surface temperature and electrical dispersion along the sensing layer. The effect of TiO_2 and ZnO semiconductors heat transfer is evaluated over the sensing layer at room temperature and different high temperatures.

2 Structure design

Gas sensors are smart devices used to sense many other gases with concentrations ranging from ppm and ppb in the presence of other low concentrations gases [34]. Although it is considered to be an apparently simple operating principle, the gas detection mechanism is quite complicated. MEMS-based gas sensors consist of two main layers as shown in Fig.1. Gas sensing performance and especially sensitivity are controlled these two layers. A chemical or biochemical interface is required to obtain sufficient sensitivity and selectivity for the analyte. This interface is called the sensing layer, this is the top layer. Gas detection mechanism is related to the change of one or more physical properties of the sensing material such as mass, elastic hardness, viscosity, electrical conductivity, and electrical permeability. The conductivity of the sensing material is expected to change according to the gas concentration. It is also desired that this change in conductivity be reversible. The performance of a gas sensor depends on the sensor configuration as well as the interaction of the sensing material with the gas. It is important to understand the interaction between the sensor material and the analyte molecules of basic sensor parameters such as sensitivity and selectivity. If this interaction is weak; sensitivity and selectivity are weakened when the sensor shows good recycling or recycling is weakened while showing good sensitivity and selectivity [35]. Another layer is the transducer layer. This layer converts the sensing analyte signals from the chemical interaction occurring in the sensing layer into an electrical signal.

Figure 1. *MEMS-based gas sensors layer structure*

Sensor specifications, for instance sensitivity, selectivity, response and recovery times, are affected by the properties of the sensing material. In this study, TiO2 and ZnO are preferred as a sensing material. ZnO has high chemical and thermal stability, piezoelectric properties. These provide excellent detection response. It has a low cost. It offers easy production and non-toxic. Thanks to these advantages, they are preferred in gas sensor applications [1]. TiO2 is also stable, low cost and non-toxic semiconductor material. It has unique electrical, optical and catalytic gas sensing material because of its wide bandgap. In smart device applications, the band structure provides superior electronic and optical properties [36]. The designed gas sensors structure is presented in Fig.2.

$LiNbO_3$ wafer is used as a substrate. On the substrate, gold electrodes are evaporated in a vacuum for electrical conductivity. Above the gold electrodes, the sensing layer is sputtered.

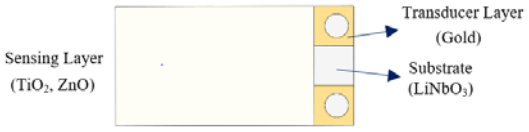

Figure 2. *Gas sensor structure*

Mechanical properties are given in Table 3. The hot plate to be used as a high heat source will be placed where the gas sensor socket in the gas detection chamber.

Table 3. *Mechanical properties of sensor structure*

Material	Size: Length x Wide (mm)	Size: Thickness (mm)	Thermal Conductivity (W/(m.K))	Density (kg/m3)	Young's Modulus (GPa)
LiNbO3[37]	6x3	0.5	5.6	4640	170
Gold [38]	6x1	1x10-4	317	19300	70
TiO_2 [39]	5x3	5x10-5	8.9	4230	230
ZnO [40]	5x3	5 x10-5	60	5676	210

3 Electrical conductivity and heat transfer analysis

The heat transfer analysis and joules heating simulation are important for observing the homogeneous heat dispersion on the surface. Homogeneous heat dispersion is one of the determining factors of sensor sensitivity. Seeing that metal oxide gas sensors work according to the resistance change principle, it is expected to be homogeneous and constant at the electrical voltage on the

sensing surface. For electrical conductivity simulation, the electrical field dispersion (E) is determined using Eq.1.;

$$E = -\nabla v \quad (1)$$

The electrical resistivity of most materials changes with temperature. To calculate electrical resistivity, a linear approximation is typically used. For electrical resistivity, (ρ) in certain temperature is determined by Eq.2;

$$\rho(T) = \rho_0(1 + \alpha(T - T_0)) \quad (2)$$

In Eq.2; ρ(T) is electrical resistivity in a certain temperature, ρ0 is electrical resistivity at 20 ºC, α is temperature coefficient at 20 ºC, T0 is 20 ºC and T is a certain temperature.
According to the electric field (E); electrical conductivity of the sensing material,(σ), current density (J) and joule

$$J = \sigma E \quad (3)$$
$$Qj = \nabla J \quad (4)$$

heating power (Qj) are calculated by Eq.3., and Eq.4.; Moreover, the heat transfer is calculated with Eq.5. The heat transfer depends on the heat flux, thermal conductivity, absolute depends on the thermal conductivity, temperature difference, and length of the body. In this equation, q, Δt, and k represent the heat flux, the temperature difference, and the thermal conductivity respectively [41] .

$$q = \frac{k.\Delta t}{L} \quad (5)$$

4 Results and discussion

4.1 Electrical dispersion

The sensing layer electrical dispersion of the gas sensor from room temperature to 573,15K is analyzed. A 9V initial voltage is applied to the gas sensor. In accordance with the resistivity of the sensor material, the average voltage above the sensing layer surface is observed and it is presented in Fig.3. At the ZnO surface, electrical dispersion has three different distinct regions.

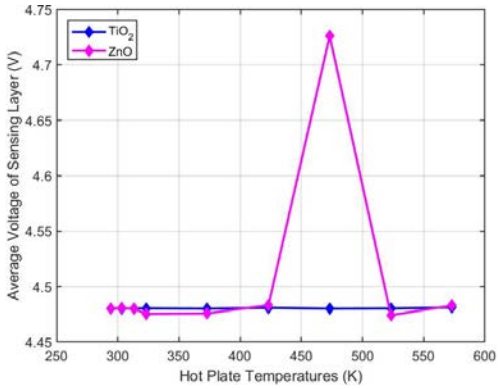

Figure 3. *Average voltage above the sensing layer (TiO_2, ZnO)*

In region I, the average electrical potential is observed steadily from room temperature to 423,15K. ZnO exhibits a negative temperature coefficient of resistance (NTCR) behavior in this region. At second region from 423,15K to 523,15K ZnO indicates a positive temperature coefficient of resistance (PTCR) behavior.

Resistivity level is the lowest in this region. In region III from 523,15K to 573,15K resistivity increases again and ZnO shows a negative temperature coefficient in this region. There are several studies about the temperature-dependent resistivity of ZnO according to NTCR and PTCR behavior.

The simulation results obtained are compatible with the literature [42], [43]. On the other hand, the TiO_2 surface electrical dispersion is observed steadily. TiO_2 shows a negative temperature coefficient from room temperature to 573,15K.

4.2 Temperature dispersion

In this simulation; absolute pressure is 1 atm. First of all, the room temperature condition is done and heat dispersion is observed. Then, high temperature conditions (323,15K, 373,15K, 423,15K, 473.15K, 523,15K, 573,15K) are created by hot plate respectively. An initial temperature (T_0=room temperature) is 294,15K and the external temperatures (T_{ext}=hot plate temperature) were applied by increasing the temperature step by step from 323,15K to 573,15K. Fig.4, and Fig.5 shows the temperature profiles of TiO_2 and ZnO sensing layers with a base substrate.

A uniform sensing layer temperature is a requirement for sensitive operation of the sensor. Figure 4 and 5 shows uniform temperature dispersion on the sensing surface at different operating temperatures. Furthermore, Fig.6. shows the comparison of surface temperature at constant electrical voltage 9V. While the temperature on the TiO_2 surface at 473,15K was 489.56 K and 569.86 K on the

ZnO surface, the temperature on the TiO_2 surface at 573,15K was 603.41 and 715.51 K on the ZnO surface.

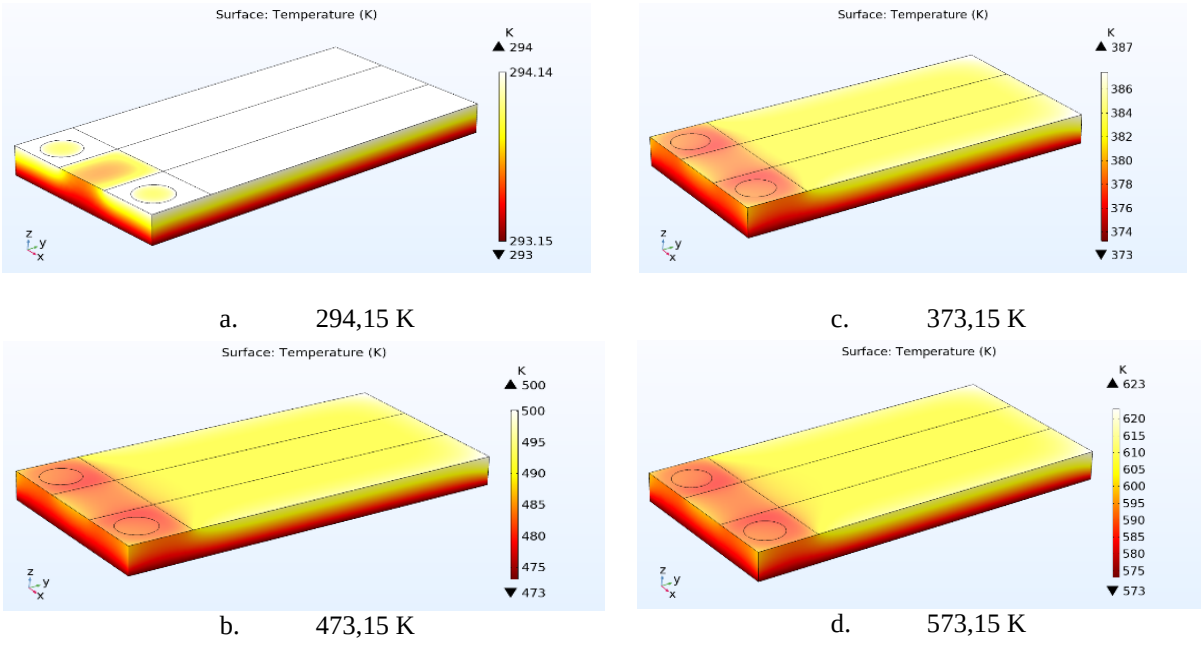

Figure 4. *Temperature dispersion in TiO_2 layer, for the temperature 294,15K (a), 373,15K (b), 473,15K (c), 573,15 K (d)*

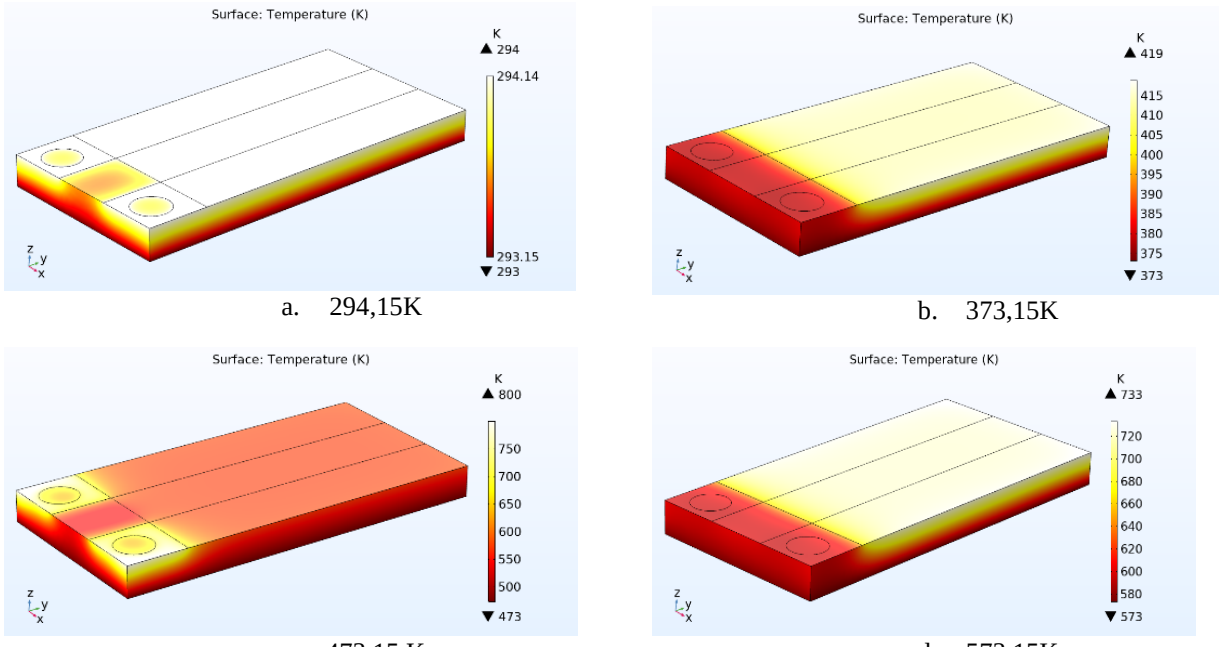

Figure 5. *Temperature dispersion in ZnO layer, for the temperature 294,15K (a), 373,15K (b), 473,15K (c), 573,15K (d)*

The comparison in Fig.6. depicts that sensing surface temperature increase on both surfaces; increased proportionally from the room temperature to 423.15 K.

When 423.15 K exceeds; the temperature increase on ZnO surface gained acceleration compared to TiO_2 surface. While the temperature on the TiO_2 surface at 473,15K was 489.56 K and 569.86 K on the ZnO surface, the temperature on the TiO_2 surface at 573,15K was 603.41 and 715.51 K on the ZnO surface.

According to the simulation results, the optimum operating temperature was determined of ZnO and TiO_2 thin films. Sensing surface temperature rises above at the 473.15K, 523.15K, 573.15K operating temperature.

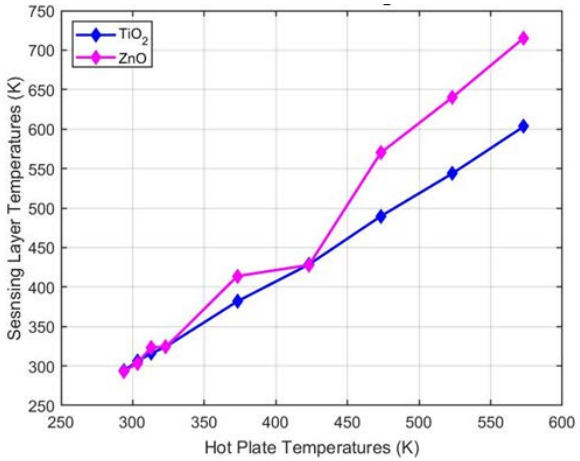

Figure 6. *Sensing layer temperature at different hot plate temperatures*

Consequently, heating inevitably occurs on the surfaces. In this case, the optimum working temperature for both thin-film structures with a thickness of 0.5 µm was determined as 423.15 K.

5 Conclusion

In this study, heat transfer analysis of the MOx-based gas sensor is discussed. Two sensing layer structures that used TiO_2 and ZnO as a material are designed and simulated. To achieve uniform heat dispersion above TiO_2 and ZnO sensing layer at room temperature and high temperature are analyzed by using FEM with COMSOL Multiphysics. The temperature profiles of sensing layers are analyzed and uniform heat dispersion was achieved in both thin films. As stated in simulation results, an optimum working temperature was determined for ZnO and TiO_2 thin films.

Our future works will be focused on the designed metal-oxide/polymer-based gas sensor at room temperature and high temperature and compared simulation results between them. Additionally, we aim to design and fabricate a gas sensor using metal oxide and metal oxide/polymer sensing layer.

Acknowledgment

This work was supported by Scientific Research Projects Coordination Unit of Istanbul Gedik University. Project number "GDK201905-14"

References

[1] V. S. Bhati, M. Hojamberdiev, and M. Kumar, "Enhanced sensing performance of ZnO nanostructures-based gas sensors: A review," *Energy Reports*, no. xxxx, 2019.

[2] K. H. Rahman and A. K. Kar, "Titanium-di-oxide (TiO2) concentration-dependent optical and morphological properties of PAni-TiO2 nanocomposite," *Mater. Sci. Semicond. Process.*, vol. 105, no. April 2019, p. 104745, 2020.

[3] R. Kumar and R. Ghosh, "Selective determination of ammonia, ethanol and acetone by reduced graphene oxide based gas sensors at room temperature," *Sens. Bio-Sensing Res.*, vol. 28, no. January, p. 100336, 2020.

[4] L. Kumar, I. Rawal, A. Kaur, and S. Annapoorni, "Flexible room temperature ammonia sensor based on polyaniline," *Sensors Actuators, B Chem.*, vol. 240, pp. 408–416, 2017.

[5] B. Mondal, M. S. Meetei, J. Das, C. Roy Chaudhuri, and H. Saha, "Quantitative recognition of flammable and toxic gases with artificial neural network using metal oxide gas sensors in embedded platform," *Eng. Sci. Technol. an Int. J.*, vol. 18, no. 2, pp. 229–234, 2015.

[6] W. H. Brattain and J. Bardeen, "Surface properties of germanium," *Bell Syst. Tech. J.*, vol. 32, no. 1, pp. 1–41, 1953.

[7] T. Seiyama, A. Kato, K. Fujiishi, and M. Nagatani, "A new detector for gaseous components using semiconductive thin films.," *Anal. Chem.*, vol. 34, no. 11, pp. 1502–1503, 1962.

[8] C. Wartelle, N. Pereira Rodrigues, M. Koudelka-Hep, and F. Bedioui, "Amperometric fluidic microchip array sensing device for nitric oxide

determination in solution," *Mater. Sci. Eng. C*, vol. 26, no. 2–3, pp. 534–537, 2006.

[9] S.-M. Park, S.-L. Zhang, and J.-S. Huh, "NO Sensing Characteristics of ZnO Nanorod Prepared by Ultrasound Radiation Method," *Korean J. Mater. Res.*, vol. 18, no. 7, pp. 367–372, 2008.

[10] Z. Zhang, C. Yin, L. Yang, J. Jiang, and Y. Guo, "Optimizing the gas sensing characteristics of Co-doped SnO 2 thin film based hydrogen sensor," *J. Alloys Compd.*, vol. 785, pp. 819–825, 2019.

[11] F. Rathgeb and G. Gauglitz, "Optical gas sensors in analytical chemistry: Applications, trends and general comments," *Encycl. Anal. Chem. Appl. Theory Instrum.*, 2006.

[12] G. Korotcenkov and B. K. Cho, "Metal oxide composites in conductometric gas sensors: Achievements and challenges," *Sensors Actuators, B Chem.*, vol. 244, pp. 182–210, 2017.

[13] C. Liu *et al.*, "A high-performance flexible gas sensor based on self-assembled PANI-CeO2 nanocomposite thin film for trace-level NH3 detection at room temperature," *Sensors Actuators, B Chem.*, vol. 261, pp. 587–597, 2018.

[14] S. Mahajan and S. Jagtap, "Metal-oxide semiconductors for carbon monoxide (CO) gas sensing: A review," *Appl. Mater. Today*, vol. 18, p. 100483, 2020.

[15] Y. De Wang, X. H. Wu, Q. Su, Y. F. Li, and Z. L. Zhou, "Ammonia-sensing characteristics of Pt and SiO2 doped SnO2 materials," *Solid. State. Electron.*, vol. 45, no. 2, pp. 347–350, 2001.

[16] S. Ummartyotin and H. Manuspiya, "A critical review on cellulose: From fundamental to an approach on sensor technology," *Renew. Sustain. Energy Rev.*, vol. 41, pp. 402–412, 2015.

[17] M. R. Vilar *et al.*, "Development of nitric oxide sensor for asthma attack prevention," *Mater. Sci. Eng. C*, vol. 26, no. 2–3, pp. 253–259, 2006.

[18] H. BISGAARD, L. LOLAND, and J. A. N. H. ØJ, "NO in exhaled air of asthmatic children is reduced by the leukotriene receptor antagonist montelukast," *Am. J. Respir. Crit. Care Med.*, vol. 160, no. 4, pp. 1227–1231, 1999.

[19] A. D. Smith and D. R. Taylor, "Is exhaled nitric oxide measurement a useful clinical test in asthma?," *Curr. Opin. Allergy Clin. Immunol.*, vol. 5, no. 1, pp. 49–56, 2005.

[20] D. R. Taylor, M. W. Pijnenburg, A. D. Smith, and J. C. de Jongste, "Exhaled nitric oxide measurements: clinical application and interpretation," *Thorax*, vol. 61, no. 9, pp. 817–827, 2006.

[21] C. Grimes *et al.*, "A sentinel sensor network for hydrogen sensing," *Sensors*, vol. 3, no. 3, pp. 69–82, 2003.

[22] M. Z. Jacobson, W. G. Colella, and D. M. Golden, "Cleaning the air and improving health with hydrogen fuel-cell vehicles," *Science (80-.).*, vol. 308, no. 5730, pp. 1901–1905, 2005.

[23] A. M. Bassam, A. B. Phillips, S. R. Turnock, and P. A. Wilson, "Development of a multi-scheme energy management strategy for a hybrid fuel cell driven passenger ship," *Int. J. Hydrogen Energy*, vol. 42, no. 1, pp. 623–635, 2017.

[24] L. Boon-Brett *et al.*, "Identifying performance gaps in hydrogen safety sensor technology for automotive and stationary applications," *Int. J. Hydrogen Energy*, vol. 35, no. 1, pp. 373–384, 2010.

[25] W. J. Buttner, M. B. Post, R. Burgess, and C. Rivkin, "An overview of hydrogen safety sensors and requirements," *Int. J. Hydrogen Energy*, vol. 36, no. 3, pp. 2462–2470, 2011.

[26] K. H. Kim, E. C. Jeon, Y. J. Choi, and Y. S. Koo, "The emission characteristics and the related malodor intensities of gaseous reduced sulfur compounds (RSC) in a large industrial complex," *Atmos. Environ.*, vol. 40, no. 24, pp. 4478–4490, 2006.

[27] H. Kimura, "Hydrogen sulfide: Its production and functions," *Exp. Physiol.*, vol. 96, no. 9, pp. 833–835, 2011.

[28] K. H. Kim, Y. Choi, E. Jeon, and Y. Sunwoo, "Characterization of malodorous sulfur compounds in landfill gas," *Atmos. Environ.*, vol. 39, no. 6, pp. 1103–1112, 2005.

[29] M. N. Hughes, M. N. Centelles, and K. P. Moore, "Making and working with hydrogen sulfide. The chemistry and generation of hydrogen sulfide in vitro and its measurement in vivo: A review," *Free Radic. Biol. Med.*, vol. 47, no. 10, pp. 1346–1353, 2009.

[30] S. C. K. Misra, P. Mathur, M. Yadav, M. K. Tiwari, S. C. Garg, and P. Tripathi, "Preparation and characterization of vacuum deposited semiconducting nanocrystalline polymeric thin film sensors for detection of HCl," *Polymer (Guildf).*, vol. 45, no. 25, pp. 8623–8628, 2004.

[31] C. Yao *et al.*, "Sub-ppm CO detection in a sub-meter-long hollow-core negative curvature fiber using absorption spectroscopy at 2.3 μm," *Sensors Actuators, B Chem.*, vol. 303, no. October 2019, p. 127238, 2020.

[32] S. H. Nimkar, S. P. Agrawal, and S. B. Kondawar, "Fabrication of Electrospun Nanofibers of Titanium Dioxide Intercalated Polyaniline Nanocomposites for CO2 Gas Sensor," *Procedia Mater. Sci.*, vol. 10, no. Cnt 2014, pp. 572–579, 2015.

[33] S. Pandey, "Highly sensitive and selective chemiresistor gas/vapor sensors based on polyaniline nanocomposite: A comprehensive review," *J. Sci. Adv. Mater. Devices*, vol. 1, no. 4, pp. 431–453, 2016.

[34] M. Imran, N. Motta, and M. Shafiei, "Electrospun one-dimensional nanostructures : a new horizon for gas sensing materials," no. 2, 2018.

[35] A. Altindal, "ORGANlK YARI iLETKEN FiLMLERiN KARAKTERiZASYONU VE GAZ SENSORU OLARAK UYGULANMASI," 1999.

[36] Z. Li *et al.*, "Resistive-type hydrogen gas sensor based on TiO2: A review," *Int. J. Hydrogen Energy*, vol. 43, no. 45, pp. 21114–21132, 2018.

[37] "Wafer LiNbO3 Properties," 2020. [Online]. Available: https://unitedcrystals.com/LiNbO3Prop.html. [Accessed: 10-Jan-2020].

[38] K. J. lesker Company, "Gold Properties." Kurt J. Lesker Company.

[39] K. J. L. Company, "Titanium Dioxide (TiO2) Sputtering Targets." Kurt J.Lesker Company, pp. 2–5, 2020.

[40] K. J. L. Company, "Zinc Oxide (ZnO) Sputtering Targets." Kurt J. Lesker Company, pp. 2–5, 2020.

[41] Comsol Multiphysics, "Heat Transfer, Comsol Multiphysics." 2020.

[42] T. K. Roy, D. Sanyal, D. Bhowmick, and A. Chakrabarti, "Temperature dependent resistivity study on zinc oxide and the role of defects," *Mater. Sci. Semicond. Process.*, vol. 16, no. 2, pp. 332–336, 2013.

[43] Y. Zhang and J. Han, "Microstructure and temperature coefficient of resistivity for ZnO ceramics doped with Al2O3," *Mater. Lett.*, vol. 60, no. 20, pp. 2522–2525, 2006.